Organic Light-Emitting Field-Effect Transistors Operated by Alternating-Current Gate Voltages**

By *Takeshi Yamao*, Yasuhiro Shimizu, Kohei Terasaki,* and *Shu Hotta*

Submitted to Adv. Mater. 2008, WILEY-VCH Verlag GmbH & Co. KGaA, Weinheim.

For further information, link to the following URLs:

http://www.interscience.wiley.com/

http://www3.interscience.wiley.com/journal/10008336/home

DOI: 10.1002/adma.

Organic Light-Emitting Field-Effect Transistors Operated by Alternating-Current Gate Voltages**

By *Takeshi Yamao*, Yasuhiro Shimizu, Kohei Terasaki,* and *Shu Hotta*

[*] Dr. T. Yamao, Mr. Y. Shimizu, Mr. K. Terasaki, Prof. S. Hotta

Department of Macromolecular Science and Engineering,

Graduate School of Science and Technology,

Kyoto Institute of Technology,

Matsugasaki, Sakyo-ku, Kyoto 606-8585 (Japan)

Fax number: +81-75-724-7800

Electronic mail: yamao@kit.ac.jp

[**] The authors thank New Material Devices R&D Center, Rohm Co., Ltd. for rendering the device substrates available to our studies. The authors thank Prof. Masahiro Yoshimoto for his valuable discussion and comments on the device operation mechanism. Thank are also due to Dr. Reiko Azumi and Mr. Satoshi Ota for their helpful discussions and suggestions on the growth of the single crystals. This work was supported by a Grant-in-Aid for Science Research in a Priority Area “Super-Hierarchical Structures” (No. 17067009) from the Ministry of Education, Culture, Sports, Science and Technology, Japan. Supporting Information is available online from Wiley InterScience.

Keywords: organic light-emitting field-effect transistor, thiophene/phenylene co-oligomer,

alternating-current gate voltage.

Organic light-emitting field-effect transistors (OLEFETs) are currently under intensive study owing to their multifunction including current modulation and light emission.[1] Such multifunction is associated with potentially wide applicability to display technology. Organic light-emitting diodes (OLEDs) constitute another class of organic light-emitting devices. Those devices require transistors for controlling their luminance. In the OLEFETs, on the other hand, the luminance can be modulated by changing only gate voltages, doing without any additional devices. Thus the display panels using the OLEFETs have the great advantage of largely reducing both the number of devices and the circuit complexity. The device performance of OLEFETs is based upon the simultaneous carrier injection of both holes and electrons into an organic semiconductor layer and their subsequent recombination. So far the OLEFETs[2–11] have been operated by applying direct-current (DC) voltages to the gate contact and between the source and drain electrodes. Within this framework several attempts were made to promote the injection and recombination of the carriers. Examples include the use of heterogeneous metal electrodes[6,8,10,11] and composite organic semiconductors.[3] These attempts, however, made the device structure complicated and an improvement was yet insufficient. Thus, the difficulty for electrons and holes to be simultaneously injected into the organic layer imposed serious restrictions on the structure and steady operation of the devices and, hence, hampered versatility of OLEFETs. This has urged us to renovate the device operation method. In this communication we propose a novel method of operating the devices that is characterized by applying alternating-current (AC) voltages to the gate electrode. This prompts the carrier injection from both the drain and source electrodes into an organic layer. Moreover, the stable metals such as gold and platinum can be used for those electrodes to inject both holes and electrons. The organic layer can freely be constructed in a desired form, e.g. a thin film or a crystal. As a result we have been successful in producing strong emissions

effectively without altering the device constitution. The devices are operated under AC gate frequencies 2–20,000 Hz of appropriate gate voltage amplitudes; stronger emissions take place with increasing gate frequencies. Detailed analyses of the electrical data allow us to distinguish two different regimes for the emission processes. This provides a powerful tool of studying the carrier injection and transport mechanisms in the organic semiconducting materials.

Amongst organic semiconducting materials thiophene/phenylene co-oligomers are counted as promising because of their unique optoelectronic properties.[5,8,12,13] Hence we have chosen for the present study one of the co-oligomers, 2,5-bis(4-biphenylyl)thiophene (BP1T);[14] see its structural formula in **Figure 1**a. The carrier mobility of the BP1T thin-film device is estimated at ~10^{-3} $cm^2\,V^{-1}\,s^{-1}$ from the normal p-channel DC operation.[15] We show in Figure 1b a schematic structure of the bottom-gate OLEFET device equipped with interdigitated electrodes of the channel length L. (A constant channel width is 8 cm.) The equivalent circuit is schematically shown in Figure 1c. Note that the “drain” and “source” electrodes are defined as injecting holes and electrons, respectively. An AC gate voltage v_G is applied with its amplitude V_G. In the phase $2\pi ft$, t and f stand for time and the gate voltage frequency, respectively. The drain–source current I_{DS} represents the current that flows in the BP1T layer.

Figure 2a compares photographs in which a thin-film device is either unlighted or lighting under an AC gate voltage application. The lighting device is being operated under a drain voltage V_D = 30 V, a source voltage V_S = –30 V and a gate voltage amplitude V_G = 40 V with the gate voltage frequency f = 20 kHz. The output light is blinking by eye at f = 2–20 Hz (see Supporting Information). The light, however, looks continuous over f = 200 Hz. Figure 2b shows the spectra of the above specific device for various f (2–20,000 Hz). The figure includes for comparison the spectra measured under DC gate voltages of –40, 0 and 40 V. Even for f = 2 Hz the intensity is significantly enhanced. The f dependence of the intensity is

shown in Figure 2c where the intensity is effectively increased with higher *f*. In Figure 2b and 2c the V_D and V_S together with V_G were the same as in Figure 2a. To further exemplify the device operations we display in Figure 2d and 2e the V_D (or V_S) dependences of the intensity at f = 200 Hz and 20 kHz, respectively. Under a fixed V_G = 40 V, the V_D and V_S were varied from 0 to 30 V at intervals of 5 V keeping $V_D = -V_S$. Although at f = 200 Hz the intensity is ignorable around low V_D, it rises suddenly at 15 V and increases with the magnitude of V_D. More importantly, for f = 20 kHz the device emits light even at zero V_D. For Figure 2**c**–**e** the intensities were determined by averaging those obtained from the spectral region 457.6–465.1 nm including the intensity maximum.

Figure 3a shows the drain–source current I_{DS} and emission intensity I_{em} as a function of the gate voltage phase for various f as parameters. The v_G varying with phase is shown as a guide in the uppermost diagram. The V_G is set for 80 V. At lower f (20–200 Hz), the major emission peak is in accordance with the dominant I_{DS} peak caused by the negative gate biases. At higher f (200–20,000 Hz) another emission peak arises near the origin (where the gate is swept from the negative to positive) and dominates with increasing f; see the arrows in the figure. Thus the peak height relationship between the abovementioned two emission peaks of I_{em} is eventually reversed.

The emission characteristics outlined above are interpreted as follows: Figure 3b schematically represents the carrier distribution in the channel that changes according to different phases within the negative gate bias region. The varying v_G is once again depicted in the uppermost diagram relative to V_D and V_S and the coordinates labeled P_1 and P_2 correspond to the carrier distribution represented by Figure 3b-1 and 3b-2, respectively. Suppose without the loss of generality we start from Figure 3b-1. When v_G becomes equal to V_S, the hole density close to the interface between the source electrode and the BP1T layer would be zero (pinch-off). At the next stage (Fig. 3b-2) electrons start being injected from the source contact into the BP1T layer and the pinch-off point (for holes) shifts toward the drain electrode with

the holes concomitantly depleted. The hole depletion takes place through either the radiative recombination, nonradiative recombination or a drift from the BP1T layer to the source electrode. The latter two processes do not produce emissions. To obtain an effective emission the holes and electrons must be made to coexist. For this the density of the electrons near the source contact should be large. This can be done by applying a large *positive* v_G, because the electron density in the BP1T layer is proportional to $|v_G - V_S|$. This large gate bias, at the same time, prompts the depletion of holes. Consequently, if the electrons are injected rapid enough before the holes would be drifting into the source, an efficient emission can be achieved. This is indeed the case with what is happening in the high *f* regime. The impact ionization may well promote the electron injection.[4a,16–18]

We believe the above processes occurring in the high *f* regime are crucial in the present device operating method. The relevant feature most prominently shows up when the gate is swept from the negative to positive (Fig. 3a). As expected applying high frequency gate biases produces the strong emissions. In this respect the observation of emissions occurring at zero V_D (Fig. 2e) implies that for the device placed in an electrically "symmetric" environment both the holes and electrons are evenly injected from the *same* contact.

With the DC operation we observed the continuous emission intensity accompanied by the continuous drain–source current. The emission occurring in the low *f* regime (typically 20 Hz in Fig. 3a) somewhat resembles that of the DC operation in that the emission intensity is significant only in the negative v_G region. In this region the transportation of accumulated holes is the dominant process and a small density of electrons is injected from the source contact to cause the relatively weak emission. In the conventional studies emissions were mostly observed in a region where $|v_G - V_D (V_S)|$ was small in contrast with the present studies, because both v_G and V_D (V_S) were set for the same polarity.[2,4a,5,8,9] Note in those conventional cases that one of the drain and source electrodes was usually grounded.

We show in **Figure 4**a photographs of a crystal device either unlighted or lighting. The

lighting device was operated under $V_D = -V_S = 60$ V and $V_G = 100$ V with $f = 20$ kHz. Line emissions above the channels are strongest at the edges and defect parts of the crystal. This results from the self-waveguided propagation of emissions in the crystal, as observed in other studies as well.[19] Figure 4b shows the relevant emission spectra for various f as against the DC operation. We used $V_D = -V_S = 50$ V and $V_G = 60$ V for a series of the AC measurements. Again the intensity increases with higher f. The emission spectra exhibit fine structures reflecting the vibronic coupling.[20]

In conclusion, the results in the present studies demonstrate that applying AC gate voltage is effective in producing the strong emissions in the OLEFETs. The device constitution is virtually unaltered and the stable metal such as gold and platinum can be used for the electrodes to inject both holes and electrons into the organic layer. This ensures the steady device performance. Moreover, this method will be indispensable to studying the carrier injection and transport mechanisms in the organic semiconducting materials. The present operation method can widely be applied to a variety of optoelectronic devices based on a variety of organic semiconductors with different morphologies (e.g. thin films and crystals), promising us the strong relevance to the future display technology.

Experimental

OLEFET device fabrication: The OLEFET devices were fabricated using BP1T by either vacuum-depositing its thin film or laminating the crystal onto the pre-made device substrates. Comb-shaped interdigitated electrodes were beforehand formed onto the substrates so as to be drain and source contacts by successively depositing Cr and Au (alternatively Ti and Pt) in vacuum on top of the SiO_2 layer (gate insulator) that covers a Si substrate (gate contact). The channel length L of the device was either 3 μm (for the case of a thin-film device) or 10 μm (for a crystal device); the channel width was 8 cm. The size of the device

was 2 mm × 2 mm. To complete the device the BP1T thin films were deposited on the device substrates under a pressure less than 5×10^{-3} Pa. The averaged deposition rate and resulting film thickness were ~0.25 nm/s and ~300 nm, respectively. In turn, the BP1T crystals (typically ~500 nm thick) were grown in vapor-phase under a dry N_2 environment at elevated temperatures (see ref. [21] for experimental details). The crystals were then laminated manually in close contact with the device substrates.

Emission measurements: The emission spectra were recorded with a multi-channel analyzer (Hamamatsu Photonics PMA-11 C7473-36) by accumulating emissions for 3 s and 5 s with the thin films and crystals, respectively. To monitor the emission intensities changing with phase, the emissions were collected with a photomultiplier tube and transferred to a digital data storage oscilloscope (Tektronix TDS 2024B). These measurements were carried out under vacuum (less than 0.5 Pa for the thin films and less than 5×10^{-4} Pa for the crystals).

Received:

Revised:

Published online:

References

[1] F. Cicoira, C. Santato, *Adv. Funct. Mater.* **2007**, *17*, 3421.

[2] a) A. Hepp, H. Heil, W. Weise, M. Ahles, R. Schmechel, H. von Seggern, *Phys. Rev. Lett.* **2003**, *91*, 157406. b) M. Ahles, A. Hepp, R. Schmechel, H. von Seggern, *Appl. Phys. Lett.* **2004**, *84*, 428.

[3] C. Rost, S. Karg, W. Riess, M. A. Loi, M. Murgia, M. Muccini, *Appl. Phys. Lett.* **2004**, *85*, 1613.

[4] a) T. Oyamada, H. Sasabe, C. Adachi, S. Okuyama, N. Shimoji, K. Matsushige, *Appl.*

Phys. Lett. **2005**, *86*, 093505. b) T. Oyamada, H. Uchiuzou, S. Akiyama, Y. Oku, N. Shimoji, K. Matsushige, H. Sasabe, C. Adachi, *J. Appl. Phys.* **2005**, *98*, 074506.

[5] K. Nakamura, M. Ichikawa, R. Fushiki, T. Kamikawa, M. Inoue, T. Koyama, Y. Taniguchi, *Jpn. J. Appl. Phys.* **2005**, *44*, L1367.

[6] J. S. Swensen, C. Soci, A. J. Heeger, *Appl. Phys. Lett.* **2005**, *87*, 253511.

[7] F. Cicoira, C. Santato, M. Melucci, L. Favaretto, M. Gazzano, M. Muccini, G. Barbarella, *Adv. Mater.* **2006**, *18*, 169.

[8] K. Yamane, H. Yanagi, A. Sawamoto, S. Hotta, *Appl. Phys. Lett.* **2007**, *90*, 162108.

[9] T. Sakanoue, M. Yahiro, C. Adachi, H. Uchiuzou, T. Takahashi, A. Toshimitsu, *Appl. Phys. Lett.* **2007**, *90*, 171118.

[10] T. Takahashi, T. Takenobu, J. Takeya, Y. Iwasa, *Adv. Funct. Mater.* **2007**, *17*, 1623.

[11] J. S. Swensen, J. Yuen, D. Gargas, S. K. Buratto, A. J. Heeger, *J. Appl. Phys.* **2007**, *102*, 013103.

[12] M. Ichikawa, K. Nakamura, M. Inoue, H. Mishima, T. Haritani, R. Hibino, T. Koyama, Y. Taniguchi, *Appl. Phys. Lett.* **2005**, *87*, 221113.

[13] F. Sasaki, S. Kobayashi, S. Haraichi, S. Fujiwara, K. Bando, Y. Masumoto, S. Hotta, *Adv. Mater.* **2007**, *19*, 3653.

[14] S. Hotta, H. Kimura, S. A. Lee, T. Tamaki, *J. Heterocycl. Chem.* **2000**, *37*, 281.

[15] T. Katagiri, S. Ota, T. Ohira, T. Yamao, S. Hotta, *J. Heterocycl. Chem.* **2007**, *44*, 853.

[16] T. Takenobu, T. Takahashi, J. Takeya, Y. Iwasa, *Appl. Phys. Lett.* **2007**, *90*, 013507.

[17] S. Tam, C. Hu, *IEEE Trans. Electron Devices* **1984**, *ED-31*,1264.

[18] P. A. Childs, R. A. Stuart, W. Eccleston, *Solid-State Electron.* **1983**, *26*, 685.

[19] a) T. Yamao, K. Yamamoto, Y. Taniguchi, S. Hotta, *Appl. Phys. Lett.* **2007**, *91*, 201117. b) T. Yamao, T. Ohira, S. Ota, S. Hotta, *J. Appl. Phys.* **2007**, *101*, 083517.

[20] S. Hotta, Y. Ichino, Y. Yoshida, M. Yoshida, *J. Phys. Chem. B* **2000**, *104*, 10316.

[21] T. Yamao, S. Ota, T. Miki, S. Hotta, R. Azumi, *Thin Solid Films* **2008**, *516*, 2527.

Figurers and figure captions:

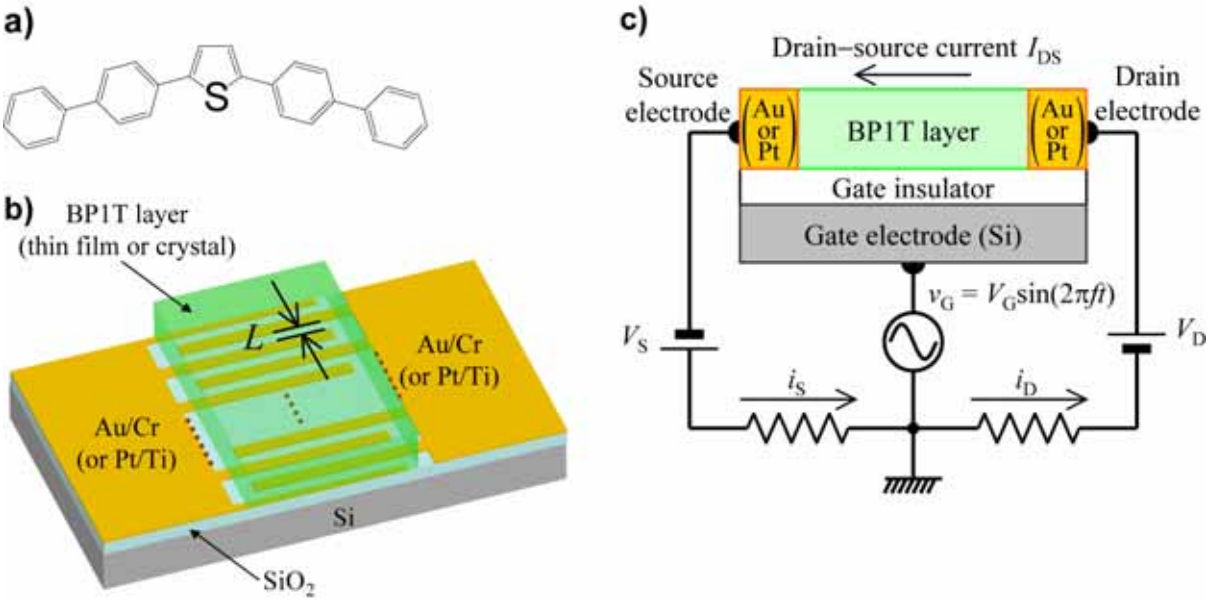

Figure 1. Schematic representations of the device structure and operation: a) Structural formula of 2,5-bis(4-biphenylyl)thiophene (BP1T) used for the organic semiconductor layer. b) Schematic structure of the OLEFET based on a thin film or a crystal. c) Schematic diagram of the electrical circuit that operates the OLEFET device. The drain and source electrodes are connected to DC power supplies. The gate electrode is connected to an AC power supply. The V_D and V_S stand for a drain voltage and a source voltage, respectively. The v_G denotes a varying gate voltage with its amplitude V_G and frequency f. Both the left-hand and right-hand side circuits each contain resistances that determine the currents i_S and i_D from voltage drops. The drain–source current I_{DS} is defined as the current that flows in the BP1T layer.

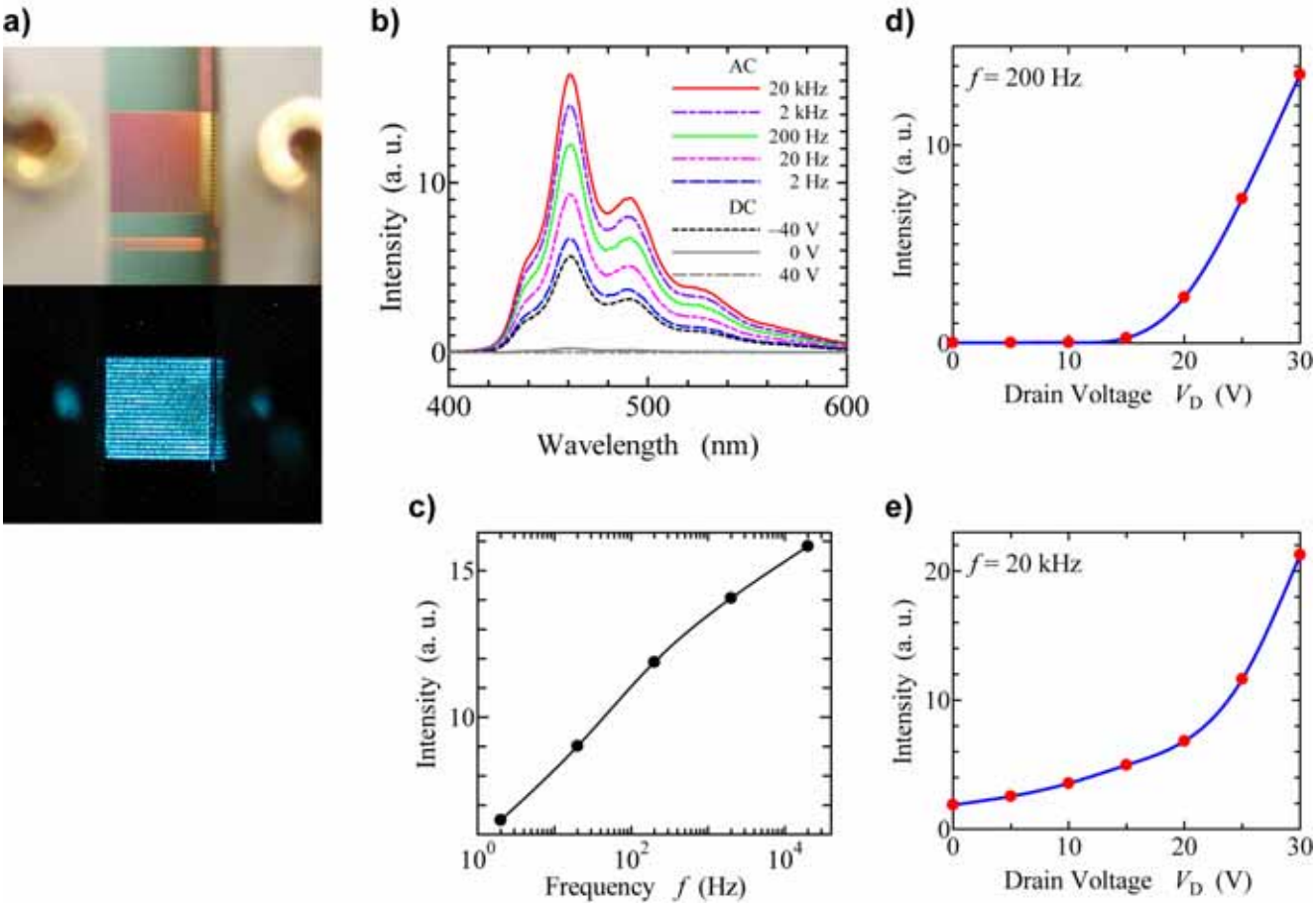

Figure 2. Emission characteristics of a thin-film device operated under AC gate biases: a) Photographs which show that a thin-film OLEFET device is either unlighted (up) or lighting in the dark under an AC gate voltage application (bottom). The central square displays a blue emission from the device that corresponds to 2 mm × 2 mm in size. b) Emission spectra from the device operated under various frequencies *f* (2–20,000 Hz). c) Frequency dependence of the intensity. d–e) Drain and source voltage dependence of the intensity for different frequencies as parameters.

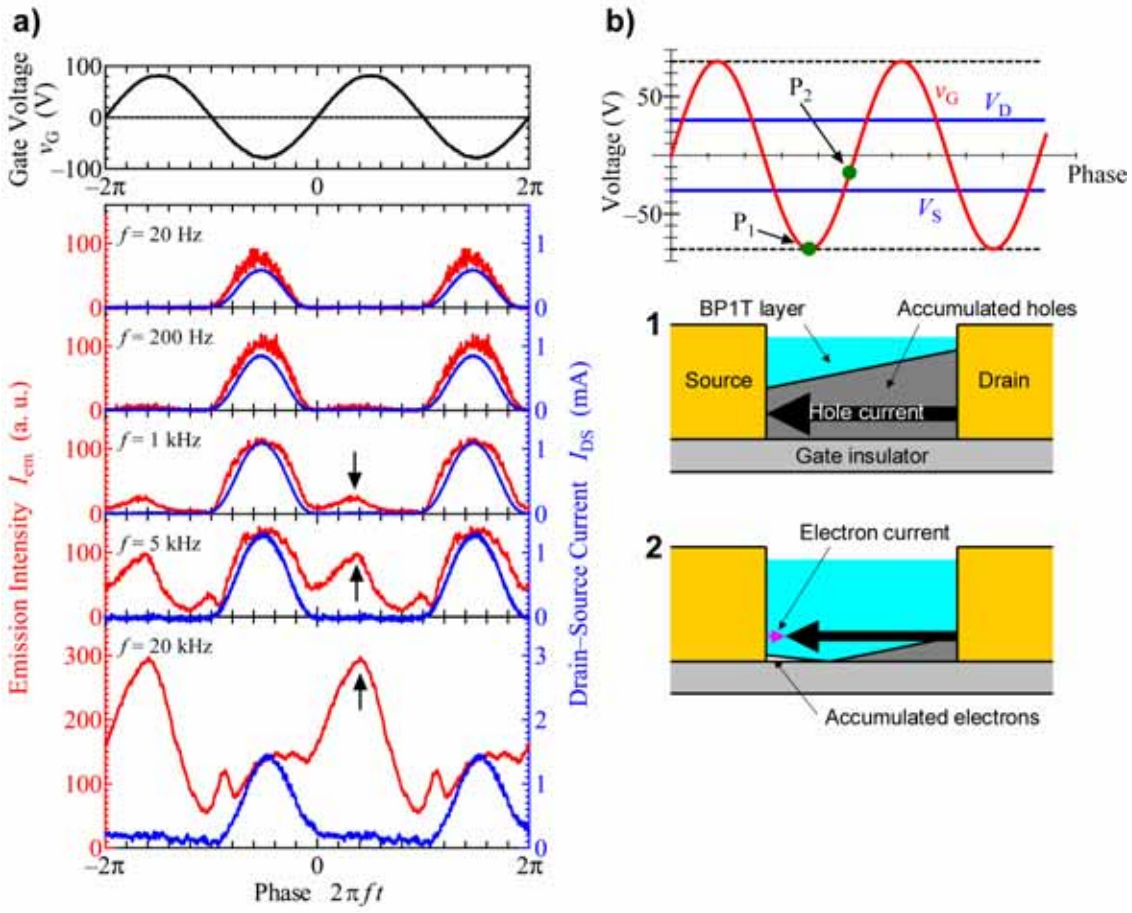

Figure 3. Drain–source currents and emission intensities relative to the carrier distribution: a) The drain–source currents I_{DS} (blue) and emission intensities I_{em} (red) are shown as a function of phase. b) Schematic diagrams of the carrier distribution within the channel at different two phases represented by P_1 and P_2. The uppermost diagram shows the locations of P_1 and P_2 with respect to V_D and V_S. The coordinate P_1 is located in the negative gate bias region where no pinch-off (for holes) occurs. Although P_2 is also positioned in the negative gate bias region, the pinch-off sets in and electrons start being injected at this point.

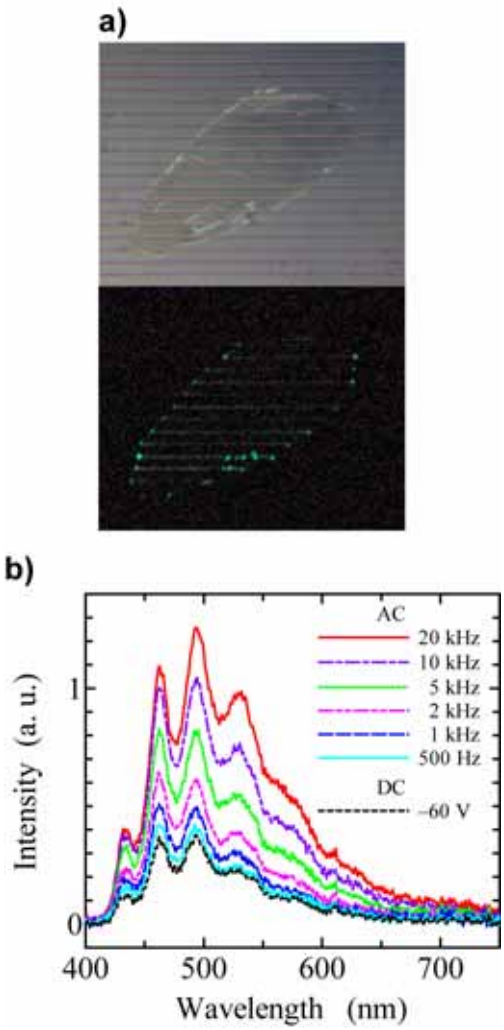

Figure 4. Crystal device and its emission spectra: a) Photographs that display a crystal device either unlighted (up) or lighting in the dark under an AC gate voltage application (bottom). The emissions are seen as lines above the channels and strongest at the edges and defect parts of the crystal. b) Emission spectra from the crystal device with increasing *f*. The data compares the AC-operated spectra with that measured under a DC gate voltage of –60 V.

The table of contents entry

Keyword (Electro-optical Materials, Light-Emitting Diode, Optically Active Materials, Semiconducting Oligomers, Transistors)

Takeshi Yamao*, Yasuhiro Shimizu, Kohei Terasaki, and Shu Hotta

Organic Light-Emitting Field-Effect Transistors Operated by Alternating-Current Gate Voltages

We propose a novel method of operating the light-emitting field-effect transistors that is characterized by applying alternating-current voltages to the gate electrode. This prompts the carrier injection from both the source and drain electrodes into an organic layer (a thin film or a crystal) without altering the device constitution. Stronger emissions are found from the device with increasing gate voltage frequencies.